**Solid Freeform Fabrication 2024: Proceedings of the 35th Annual International Solid Freeform Fabrication Symposium – An Additive Manufacturing Conference**
**Reviewed Paper**

# Novel Powder Feed Mechanism for convection of high-cohesion, sub-20-micron powders in Directed Energy Deposition

John Byers*, Adam Eungard*, Joe Jafari*, and Dr. Jennifer Bennett*
*Department of Civil and Mechanical Engineering, United States Military Academy – West Point, NY 10996

## Abstract

Functionally graded material (FGM) ceramics are a promising material for thermal applications to reduce the stress concentrations due to different thermal expansion coefficients at dissimilar material joints. Directed Energy Deposition (DED) enables processing of these FGMs by varying composition during deposition. However, ultra-high temperature ceramics, such as Titanium Diboride, cannot currently be deposited by DED. The boron powder used exhibits higher cohesion, lower density, and smaller particle sizes than traditional DED powders resulting in an inability to manufacture components using this powder. A feed system was developed by combining a feed screw and powder agitator to facilitate the delivery of boron powder to the mixing chamber of DED systems at precise and variable feed rates. The feed system successfully conveyed boron powder at variable rates enabling control over percent composition of boron and titanium to create a FGM. However, the feed mechanism failed to reliably transport powders with an average particle size below 10 microns. More research must be done to determine other feed system additions to better convey these powders such as system vibration, extensive preheating to eliminate moisture, and pressurized powder input.

**Keywords:** Additive Manufacturing, Directed Energy Deposition, Reactive Laser Deposition

## Introduction

FGMs are a rapidly growing branch of materials science research due to their ability to persevere the beneficial properties of constituent elements [1, 2]. Previously composite materials were developed to attain uniform composition and properties, for specific applications in many engineering fields [3]. However, the restricted use of traditional homogenous engineering materials including pure metals, alloys, polymers, ceramic, and traditional composites, means new materials must be fabricated to meet challenging applications requiring optimal performance in traditionally opposing mechanical properties such as heat resistance, toughness, ductility, and hardness. The creation of novel composites using a functionally graded structure across a material cross section as seen in Figure 2, could offer the traditional advantages of two separate material classes, determined by which material had a higher percent composition in that region of the component [4]. For example, advances in one branch of FGMs, Ceramic Metal Composites (CMCs), have produced graded components capable of offering the extreme temperature resistance and hardness of modern

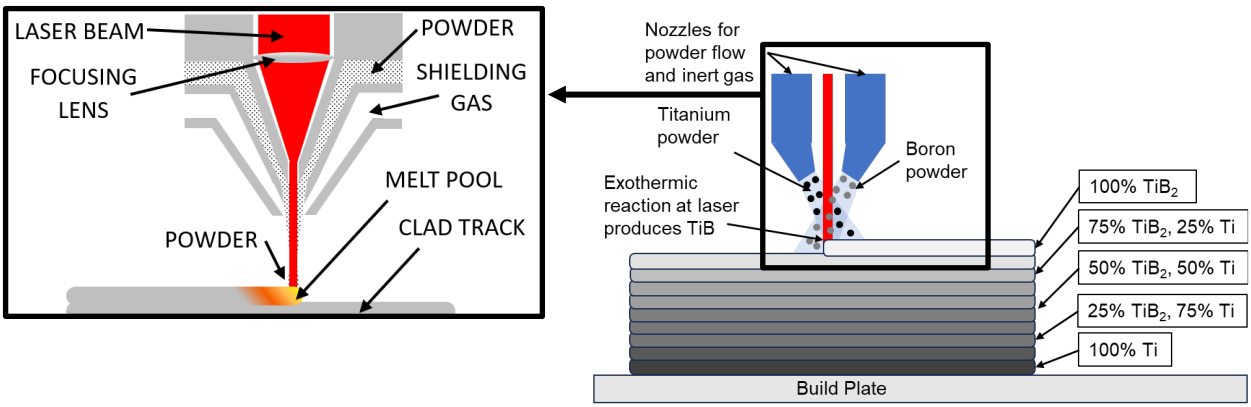


Figure 1: Diagram of DED manufacturing a functionally graded part with a detailed print head schematic shown on the left

ceramics and the toughness and ductility of metals. Previously these applications used two dissimilar materials bound together using mechanical fastens or adhesives to gain the beneficial properties of both materials. However, these binding techniques often fail in certain applications, especially those which undergo extreme heating, wear, or corrosion [5]. Additionally, the distinct material boundary creates significant stress concentrations, especially under extreme heating due to dissimilar thermal expansion coefficients. Using the novel approach offered by FGMs, this material boundary is now graded across a component, distributing stress across the cross section, increasing the survivability of resulting components. These materials are impossible to produce using traditional fabrication techniques, however new advances in additive manufacturing have created processes which can fabricate components with graded compositions due to their layer wise build process. DED is a rapidly growing metal additive manufacturing process that can produce lightweight, complex, and multi-material components as well as repair components and apply coatings [6-9]. In this process, pneumatically conveyed powder is deposited into a melt pool created on the substrate with a laser. As the deposition head and substrate move in relation to each other, the pool solidifies into clad tracks which form a component through layer-wise construction as seen in Fig. 1. Additionally, this process can reach the activation energy of the titanium diboride ceramic formation reaction through reactive laser sintering. The triggering of the exothermic formation reaction through the laser activation energy will allow the ceramic to reach the required density for adequate performance. Traditionally manufactured ceramics require post processing using a hot press, which applies immense heat and pressure to reach the required ceramic density for adequate performance. This requirement has previously limited achievable geometries, a limitation which is eliminated using reactive laser sintering via DED. This research focuses on the production of titanium and titanium diboride FGMs, due to titanium's strength to weight ratio and titanium diboride's excellent performance at high temperature combined with its high toughness compared to other ceramics. However, due to the physical properties of pure amorphous boron powder required to produce the ceramic on the build plate, namely its high-cohesion, small particle size (~10 μm), and decreased density, current DED feed mechanism are unable to convey it. As such this paper explores the design and development of a prototype feed mechanism for use with light weight, high-cohesion, and small particle size powders to allow for the creation of FGMs utilizing DED. This feed mechanism will utilize a screw feeding mechanism to consistently deliver boron, combined with a powder agitator to ensure constant dynamic flow of powder to prevent bridging and clumping in the material reservoir.

## Methodology

*2.1 Powder Testing*

To achieve integration of ceramic powders into existing DED machinery, it was necessary to characterize the materials of interest to determine their flowability and density. The feed mechanism will be designed to convey amorphous boron carbide powder however due to its high cost; an analogous boron carbide powder was selected for the purpose of testing. Additionally, as boron carbide is marketed as an abrasive grit it is commercially available in more specific particle size ranges allowing for measuring of mechanism performance across average specific particle sizes. Boron carbide was obtained in the following average particle sizes: 3, 6.5, 9.3, 12.8, 17.3, 22.8, 29.2, 36.5, and 44.5 microns. Three powder characterization tests were run on the four separate powder types consisting of pure boron, boron carbide, titanium, and stainless steel. The last two powders were included to provide a baseline standard for powders that are commonly utilized in DED manufacturing and conveyed by current feed mechanisms. The powder characterization tests consisted of Hall and Carney flow ratings, Hausner Ratio, and Compressibility Index.

The first test conducted was Hall and Carney flow according to ASTM B964. The Hall and Carney flow tests measure the time for 50 grams of powder to pass through a brass funnel with a 2.5- and 5-mm aperture respectively. This test can be conducted both dynamically and statically to provide additional information into the flow characteristics of the material. The traditional DED materials were characterized using this method, however due to boron's high cohesion and light weight, it failed to flow through either aperture under both static and dynamic conditions. As a result, this testing only was possible for titanium and stainless-steel powders. This inability to freely flow through a funnel demonstrated by both the amorphous boron and boron carbide again suggests that these powders would not be properly conveyed by current DED feed mechanisms.

To conduct the testing for Hausner Ratio and Compressibility Index, approximately 50 grams of powder was added to a graduated cylinder and the exact mass and initial bulk powder volume ( ) recorded. Using these values, the untapped or bulk powder density was then calculated before the powder underwent compression. The powder was then compressed using a 15-gram weight dropped from a height of 15 cm for a total of 50 taps. Upon the completion of these taps, the final volume ( ) was recorded to determine tapped bulk density. With the initial and final volumes, the Hausner Coefficient and Compressibility Index were calculated using Equations 1 and 2 respectively.

$$= — \quad (1)$$

$$C = ——— \quad (2)$$

Because both flowability metrics utilize the same variables, their results are proportional to each other. A Hausner Coefficient indicating excellent flow will have a corresponding Compressibility Index that also indicates excellent flow. These ratios measure the change in volume and percent compression of a sample.

Figure 2: Hall Flowmeter device

The final powder characteristic measured in this study is the angle of repose. This testing produces a value that is required to calculate the mass flow rate of a horizontal powder screw as seen in Equation 4. This equation is used to determine the required speed for the prototype based on the powder being conveyed. Angle of repose testing was only conducted on the amorphous boron since this is the material that the prototype is designed to convey. The angle of repose test reflects a powder's propensity to exhibit shear against other grains of the same powder. Shear impacts a powder's tendency to clump up or bridge when faced with a small opening. The angle of repose testing was conducted with a Hall Flowmeter to determine maximum sustainable powder angle. Powder flow was halted, and maximum angle recorded once the cone of powder began to collapse. A set of calipers was used to measure the width and height of the pile as seen in Figure 3, before calculating the maximum angle using Equation 3 [10].

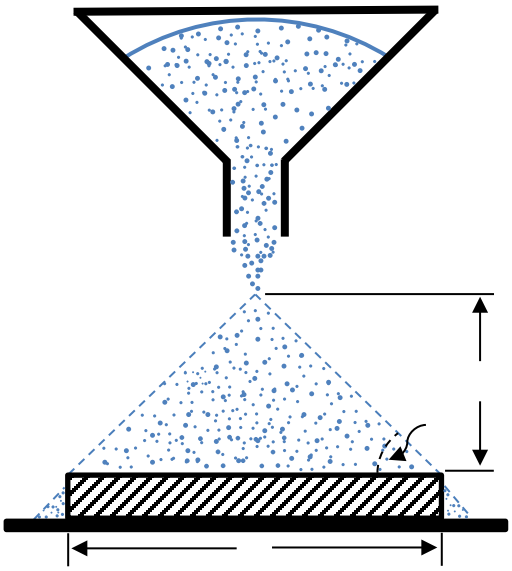

Figure 3: Diagram of angle of repose apparatus

$$= \tan \frac{2}{} \qquad 3$$

*2.2 Design*

Early deliberation over powder conveyance methods ruled out pressurized gaseous flow due to the lightweight and high cohesion of the boron in question. The lightweight nature and high cohesion combine to result in high friction and clumping along the path of travel, resulting in unpredictable and poor flow. Initially, a vertical screw conveyor was proposed to combine gravity feeding with a controlled screw speed. Following the Hall and Carney Flowmeter testing this

option was ruled out due to the powder bridging observed with boron-based powders which became more pronounced with smaller particle size. Due to the failure of a circular funnel, a horizontal screw feeder was proposed. Using a horizontal screw feeder allowed for a larger funnel aperture due to a rectangle opening as opposed to a circular opening. This horizontal screw feeder could facilitate precise and variable powder deposition through altering of screw rotational speed.

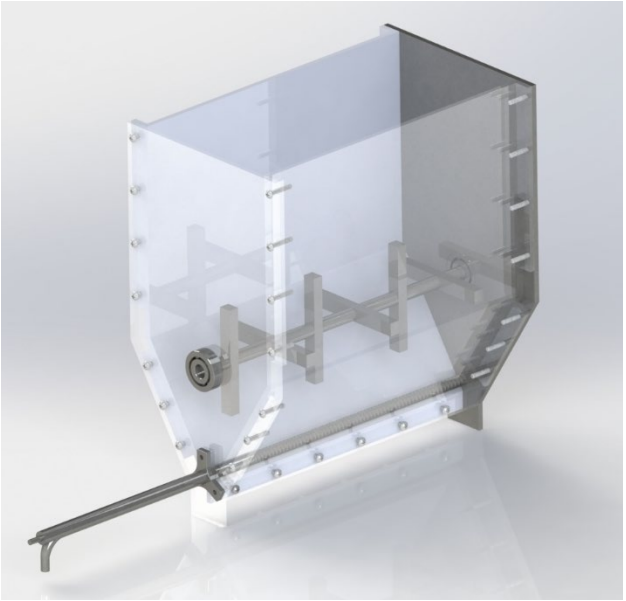

Figure 4: A SolidWorks render of the feed system with agitator and feed screw shown

As shown in Figure 4, powder is initially staged within a large rectangular hopper. An agitator in the center of the hopper will ensure powder dynamic powder motion, preventing bridging of the powder, allowing it fall evenly onto the screw at the bottom of the enclosure. The screw feeds into an enclosed pipe that protrudes from the hopper and carries the powder to an export port. At that point, pressurized argon is feed into the screw from above, forcing the powder through on output nozzle at the bottom of the pipe and into vinyl tubing. This tubing will then convey the powder through argon flow into a mixing chamber, where it will combine with titanium, ultimately outputting a homogenous mixture that facilitates reactive sintering of titanium diboride on the build plate. At the build plate this titanium diboride will be graded with pure titanium, which is being conveyed into the melt pool from a separate powder nozzle. The agitator and screw are both geared to a motor behind the hopper which is controlled by an Arduino Nano microcontroller. This design maximizes user control over the speed of the screw through a manual and autonomous mode. In manual operation, most useful for prototype testing, screw speed is controlled via a potentiometer and the rotational speed is displayed on an LCD output screen. In autonomous operation, the screw speed can be set at a constant rate or at varying rates with specified durations to facilitate gradual variation over the construction of a component.

The performance of the screw conveyor was governed by Equation 4.

$$Q = 250\pi * D^2 * S * N * \alpha * \rho * C \quad (4)$$

In this equation, Q is the screw capacity in g/min. D is the diameter, S is the screw pitch, N is the screw speed, $\rho$ is the powder bulk density, $\alpha$ is the loading ratio, and C is the inclination correction factor (1 for a horizontal screw). The screw capacity can also be conceptualized as the mass flow rate. The screw speed N is the only variable. The diameter, while modified during testing, was ultimately fixed at 0.75 inches. Loading ratio $\alpha$ is dependent on the angle of repose testing obtained during the powder characterization phase. It is given by Equation 5 [11].

$$\tan \quad = \frac{\quad}{\alpha} \qquad 5$$

The final design was constructed from stainless steel to improve cleanliness and avoid cross-contamination between materials. It also offers high corrosion resistance, which promotes longevity. The hopper consisted of three pieces of sheet metal, the front, rear, and side walls that wrap around the screw. Gaps in between these sheets were sealed with rubber. The agitator and screw were affixed to the rear plate with press fit bearings. A collar screwed to the front plate supported the screw pipe housing. A hole was drilled and tapped at the end of the pipe to support the argon flow nozzle. At the bottom of the pipe the vinyl hosing was attached to provide a pathway for the powder to the mixing chamber. Behind the rear plate, the screw and agitator are geared to a motor controlled by the Arduino Nano. In manual mode, a red LED is illuminated. In autonomous mode the speed can be modified to accommodate complex part geometries, longer times at certain compositions (e.g. 25% $TiB_2$), and preset storage.

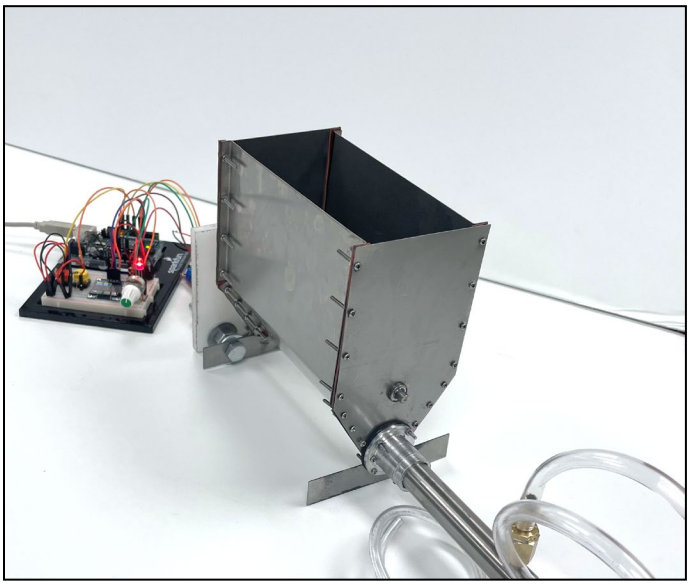

Figure 5: Final Prototype

### *2.3 Target Mass Flow Rate Analysis*

When determining the target mass flow rate for the prototype powder feeder, typical flow rate ranges for DED printing were considered to establish a baseline target range of 5-20 g/min. As these flow rates are representative of total powder delivered to the build plate for single material printing, they were then adjusted to the application of printing FGMs. The maximum mass flow rates required by a single nozzle in this printing method would be seen at the first or last layer printed where the material composition would be pure boron carbide of pure titanium. Tailoring the feed rates required in these layers to the conveyance of pure boron requires consideration of the material composition of titanium diboride. As this ceramic is typically composed of only 31% boron by mass, the target feed rate for the prototype was set at 2-6 g/min. However, given the weight and size of boron powder compared to typical DED materials, approximately 6.6 and 2.5 times less than titanium respectively, there is increased likelihood of powder failing to reach or penetrate the surface tension of the melt pool. Previous papers have defined the melt pools as incredibly violent regions that are significantly impacted by kinetic impacts, increasing the likelihood that due to its weight, boron will struggle to reach the target area [8]. The target mass flow rate for the prototype was increased by 50% to allow for adjustment pending future on successful delivery of comparatively light powders to the melt pool. This was done to account for expected powder loss due to both these differences when compared to traditional DED powders. From these considerations the target mass flow rate set for the prototype was 3-9 g/min, with a goal flowrate of 9 g/min at maximum motor speed.

### *2.4 Simulation Processing*

Proof of concept simulation was performed using LAAMPS Improved for General Granular and Granular Heat Transfer Simulations (LIGGGHTS). This software allows for inclusion of particle sizes, Poisson ratios, and specific powder characteristics that would be crucial to analyzing the powder's effects on the screw feeder system [9]. A baseline screw feeder design was utilized to determine effectiveness of the chosen method prior to fabrication of the final prototype. The resulting LIGGGHTS simulation results were visualized on Paraview, where the particle size, speed, and gravitational effects could also be adjusted. Although this model was not benchmarked against experimental results using angle of repose testing to determine accuracy of predicted cohesion, the simulated powder was assigned high cohesive factor typical of fine powders. This simulation was utilized as a proof of concept to determine areas of likely failure in the prototype design and determine the need for additional mechanism to aid powder flow (agitators, vibration, pressurized input eg.). An example of simulated flow visualization can be seen below.

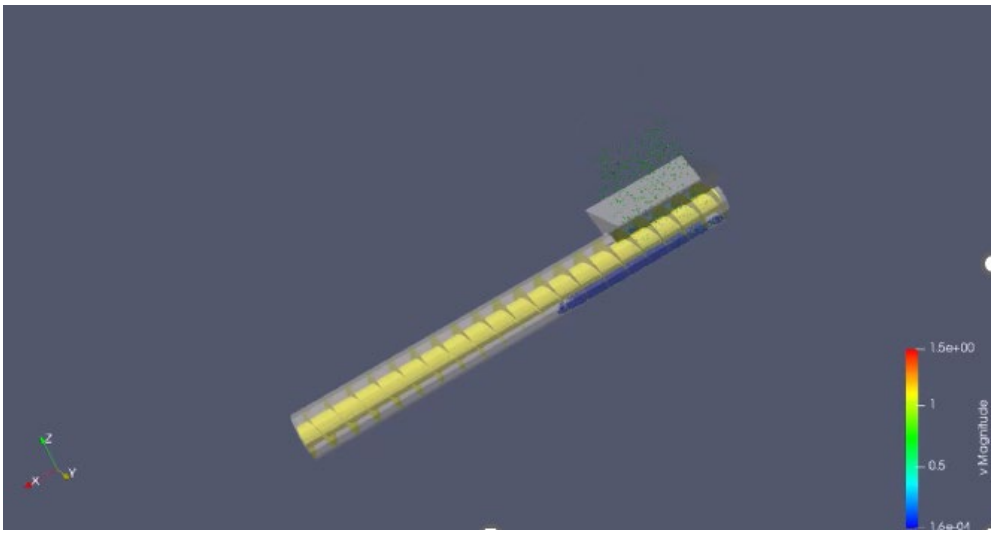


Figure 6: LIGGGHTS Simulation of Horizontal Screw feeder

## Results and Discussion

### *3.1 Powder Characterization Results*

When considering the redesign of the powder feeding mechanism used in DED system for boron conveyance, the specific powders had to first be characterized and compared to traditional DED materials. To define the flow of these materials, several tests were conducted to produce coefficients related to ease of flowability. Powder compression tests were performed to produce Hausner Coefficients and Compressibility Indexes for each powder. In this test 50 grams of powder were added to a graduated cylinder and the bulk volume was measured. Then the powder was compressed through 50 taps of a 15-gram weight dropped from 15-cm. The final volume was recorded, and the two coefficients were calculated using Equations 1, 2. These coefficients account for the compression of a powder which correlates to the cohesion and particle size of the material. Each coefficient categorizes the ease of flowability into regions of flowability. The results of this testing are seen in Figure 10, where the coefficients are plotted against the freely settled bulk density of the powders.

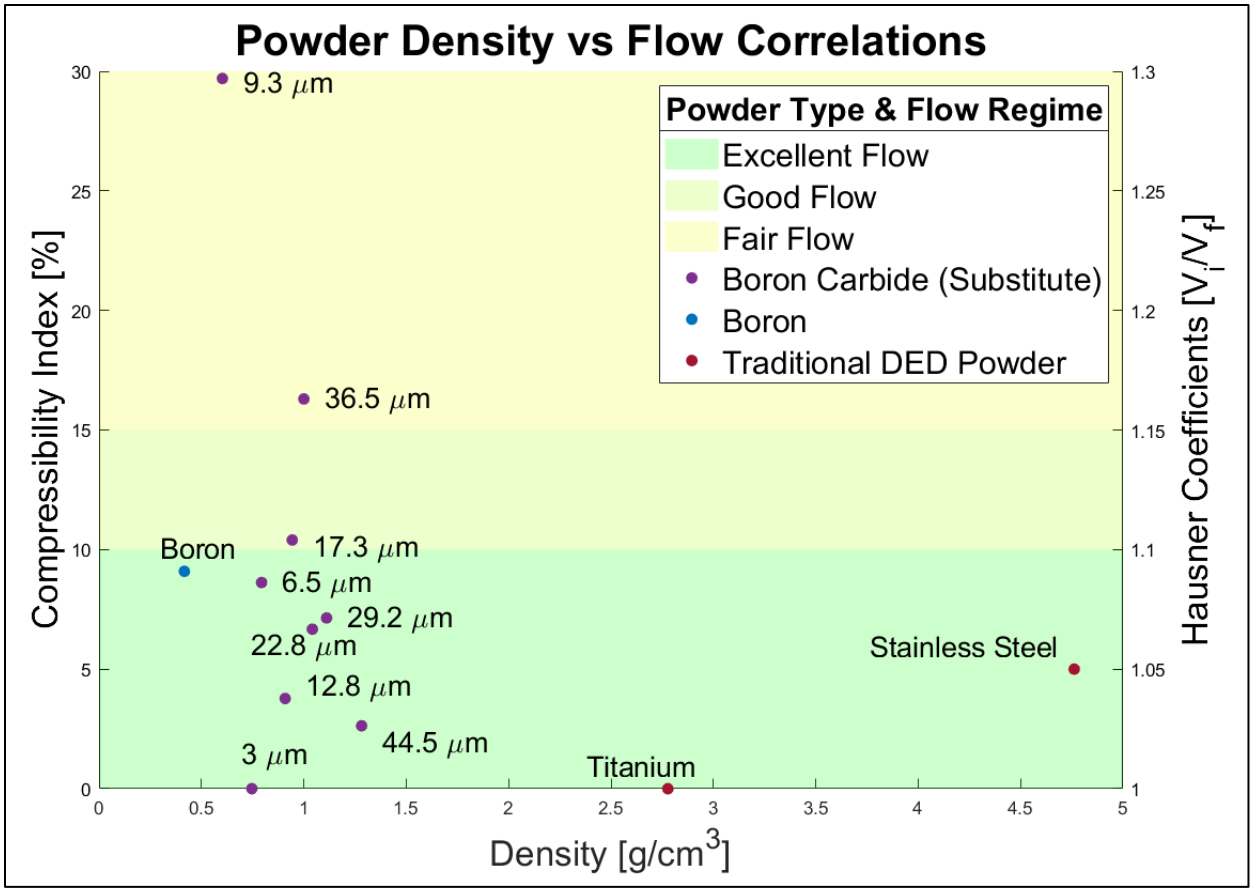


Figure 7: Powder Flowability Testing Results

The results from this testing demonstrated that both the pure boron and boron carbide powders demonstrated higher Compressibility Indexes and Hausner Coefficients. The titanium and stainless-steel DED powders demonstrated freely settled bulk densities of 2.78 and 4.76 grams per cubic centimeter respectively. Comparatively the pure boron was approximately 85% lighter than titanium with a bulk density of 0.42 grams per cubic centimeter. The boron carbide powders exhibited slightly higher densities, yet still demonstrated densities that were approximately 54-73% lighter than titanium. Despite most of the tested boron particle sizes falling in the excellent flow region, the significantly higher compression and lighter densities suggest that they will be significantly more challenging to convey than traditional DED powders. This is supported by the experimental findings that both the pure boron and smaller particle sizes of boron carbide failed to pass through a funnel with a 5-mm aperture (Carney Flowmeter Funnel) due to cohesion and density.

*3.2 Prototype Feed Mechanism Feed Rate Results*

Testing of the prototype feed mechanism was conducted to validate the accuracy and consistency of powder feed rates. Boron carbide powders at 9.3, 22.8, and 44.5 µm Average Particle Size (APS) were tested to ensure consistent conveyance across the range of potential particle sizes that will be used in the system. Five trials were conducted at 95, 70, and 50 RPM motor speeds for each of the three powders. Powder was added to the hopper until the surface

was 2 cm above the top of the feed screw. The system was run for 10 seconds during each trial and the weight of the powder dispensed was measured, before it was converted to a mass flow rate in units of grams per minute. The results of this testing can be seen below in Figure 8 and Table 1.

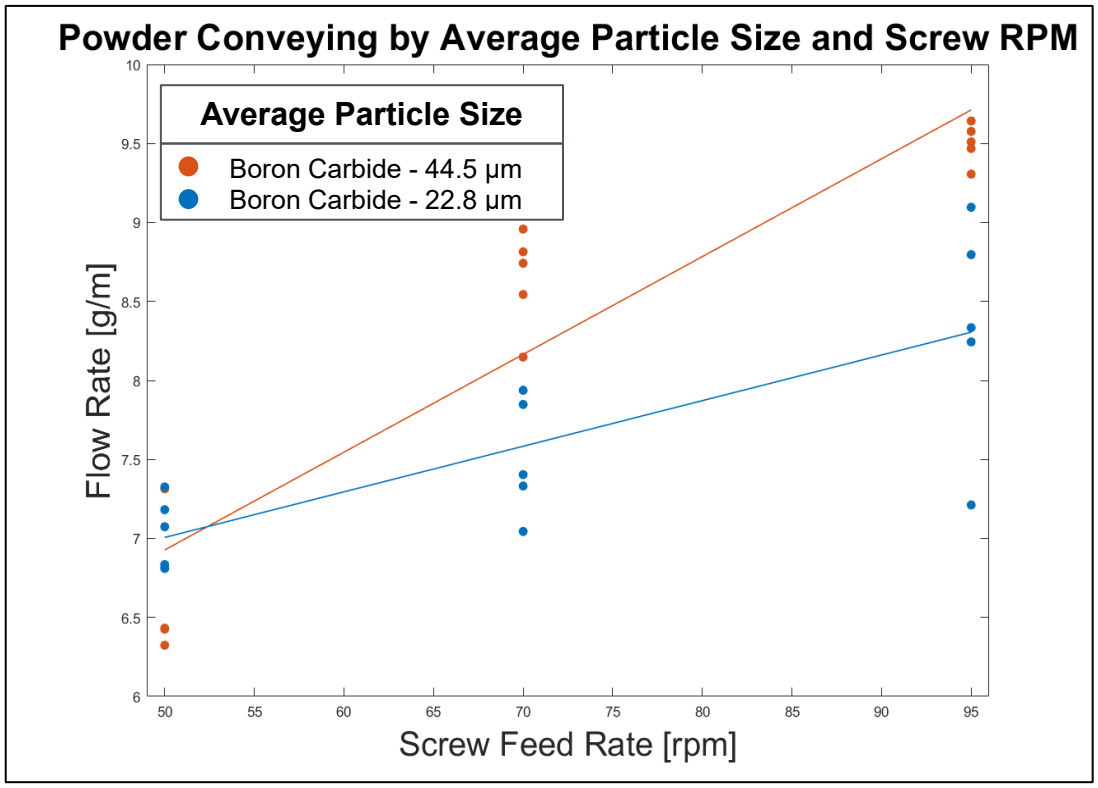


Figure 8: Screw Feeder Flow Results from Powder Conveying

| Screw Speed [rpm] | Average feed rate [g/m] | Variance |
|---|---|---|
| Boron Carbide F240 - 44.5 µm | | |
| 90 RPM | 9.50 | 0.01 |
| 70 RPM | 8.64 | 0.13 |
| 50 RPM | 6.66 | 0.08 |
| Boron Carbide F360 - 22.8 µm | | |
| 90 RPM | 8.34 | 0.41 |
| 70 RPM | 7.51 | 0.11 |
| 50 RPM | 7.05 | 0.04 |
| Boron Carbide F600 - 9.3 µm[a] | | |
| 90 RPM | 3.10 | 7.02 |

[a]This powder demonstrated high variability across each trial due to high-shear, moisture content, and high compressibility.

Table 1: Powder Dispensing Results from Screw Feeder Speed Variations

Referring to Table 1 the 44.5 μm boron carbide displayed the most ideal flow of the three tested powders. At a maximum motor speed of 95 rpm, the observed average mass flow rate across five trails was 9.5 g/min. This is above the required upper mass flow rate range of the prototype which was 9 g/min. As seen in Figure 8 this powder also followed a roughly linear relationship between mass flow rate and motor speeds aided in ease of parameter adjustment for a DED system. This powder displayed the lowest variance between the five trials for each tested motor speed, with a maximum value of 0.13 g/min.

The 22.8 μm powder performed second best with a mass flow rate of 8.34 g/min at maximum motor speed. This powder also displayed a roughly linear relationship between motor speed and mass flow rate. However, the variance between the five trials also increased to a maximum of 0.41 g/min, likely due to the reduced particle size and associated increased cohesion leading to more unpredictable bulk powder flow.

This relationship is supported by the results of the 9.3 μm powder, which can be seen in Table 1. The average mass flow rate for this powder was 3.1 g/min, failing to reach the target mass flow rates of 9 g/min at maximum motor speed. Interestingly, each trial mass flow rate decreased significantly compared to the previous one. The sequential mass flow rates for each trial were 7.52, 4.65, 1.85, 1.16, and 0.32 g/min. The most likely reason for this reduction in flow rate is the high compressibility and cohesion of this powder, a result of its small APS. Additionally, once particle size drops below 10 μm, the powder begins to resist gravitational flow, likely adding to this effect. During testing this powder was compressed substantially by the feed screw as opposed to being uniformly conveyed. As the powder was compressed, flow rates decreased, and material was deposited in small, compressed clusters instead of a loose powder. Although not analyzed in this study, powder compression would significantly reduce the effectiveness of the mixing chamber and could result in non-uniform material composition within layers. These inconsistent flow effects resulted in an extremely high variation between trials of 7.02 g/min. Considering these results, when using boron or similar materials in composite FGM DED manufacturing, APS should be maintained above the 10 μm threshold to increase consistency and uniform flow to the build plate.

## Conclusion

This research was centered around the goal of redesigning the powder delivery system in DED printing to allow for the use of extremely light, high shear powder necessary for ceramic gradient printing. The design prototype effectively manages powder delivery rate at smaller particle sizes; however, it was unsuccessful when tested with the smallest particle size ranges between 1-10 microns. The combined effects of the density and cohesion resulted in stalling of the motor as powder adhered to the tube walls and locked the rotation of the feed screw. At larger particle sizes above 20 microns the screw conveyor achieved consistent powder flow to the build plate at the rate needed to facilitate ceramic printing. The mass flow rate of powder fell within the expected range of DED powder flow when accounting for final composition of the desired Titanium Diboride. While features such as the agitator effectively prevented powder from bridging in the hopper, overcoming boron's low density and high sheer especially at lower particle will require additional modifications and preprocessing steps. Increasingly powder size through deliberate microscopic material clumping to attain sizes in the range of 20 to 50 microns would be most desirable, while the addition of a pressurized input and extensive powder baking could also reduce feeding issues. Finally, more exact machine tolerances will reduce chances for stalling in the system by minimizing gaps that allow for buildup of powder at the finest range of APS. In future work pressurized argon flow will be added to ensure the powder, once fed into the system is able to travel to a mixing chamber where it will be combined with the titanium powder. Further testing is required to determine whether variations in flowrate on the millisecond scale caused by piecewise feed screw powder deposition will result in inaccurate composition across gradient components. Future research should also examine integration with the mixing unit to ensure homogenous combination of the titanium and boron before delivery to the build plate. Although unsuccessful below 10 microns, the prototype feed mechanism successfully conveyed light, high-shear, and small powders as an alternative to traditional DED feed systems.

## References


[1] B. Saleh *et al.*, '30 Years of functionally graded materials: An overview of manufacturing methods, Applications and Future Challenges', *Composites Part B: Engineering*, vol. 201, p. 108376, Nov. 2020.

[2] V. Shanmugam *et al.*, 'The mechanical testing and performance analysis of polymer-fibre composites prepared through the additive manufacturing', *Polymer Testing*, vol. 93, p. 106925, Jan. 2021.

[3] G. F. Aynalem, 'Processing Methods and Mechanical Properties of Aluminium Matrix Composites', *Advances in Materials Science and Engineering*, vol. 2020, no. 1, p. 3765791, Jan. 2020.

[4] S. Nikbakht, S. Kamarian, and M. Shakeri, 'A review on optimization of composite structures Part II: Functionally graded materials', *Composite Structures*, vol. 214, pp. 83–102, Apr. 2019.

[5] R. Viswanathan and J. Stringer, 'Failure Mechanisms of High Temperature Components in Power Plants', Journal of Engineering Materials and Technology, vol. 122, no. 3, pp. 246–255, Feb. 2000.

[6] Bennett J., Garcia D., Kendrick M., Hartman T., Hyatt G., Ehmann K., You F. & Cao J. (2019) "Repairing automotive dies with directed energy deposition: industrial application and life cycle analysis" Journal of Manufacturing Science & Engineering, vol. 141, no. 2.

[7] Bennett J., Liao H., Buergel T., Hyatt G., Ehmann K. & Cao J. (2021) "Towards Bi-Metallic Injection Molds by Directed Energy Deposition" Manufacturing Letters, vol. 27, pp. 78-81.

[8] Bennett J., Webster S., Byers J., Johnson O., Wolff S., Ehmann K., & Cao J. (2022) "Powder-borne porosity in directed energy deposition" Journal of Manufacturing Processes, vol. 80, pp. 69-74.

[9] Christoph Kloss, Christoph Goniva, Alice Hager, Stefan Amberger, Stefan Pirker "Models, algorithms and validation for opensource DEM and CFD-DEM", Progress in Computational Fluid Dynamics, An Int. J. 2012 - Vol. 12, No.2/3 pp. 140 – 152.

[10] "Screw conveyor design calculation - an Engineering Guide." Accessed: May 09, 2024. [Online]. Available: https://powderprocess.net/Equipments%20html/Screw_Conveyor_Design.html

[11] Y. Kobayashi, S. Kim, T. Nagato, T. Oishi, and M. Kano, 'Feed factor profile prediction model for two-component mixed powder in the twin-screw feeder', *Int J Pharm X*, vol. 7, p. 100242, Mar. 2024.